

Supporting information

Aggregation-induced emission fluorophores based on strong electron-acceptor 2, 2'-(anthracene-9,10-diylidene) dimalononitrile for biological imaging in the NIR-II window

Zhicheng Yang, ^{‡a} Xiaoxiao Fan, ^{‡bc} Xianglong Liu, ^a Yanmeng Chu, ^d Zhiyun Zhang, ^a Yue Hu, ^d Hui Lin, ^{*b} Jun Qian ^{*bc} and Jianli Hua ^{*a}

^aKey Laboratory for Advanced Materials, Joint International Research Laboratory for Precision Chemistry, School of Chemistry and Molecular Engineering, East China University of Science and Technology, 130 Meilong Road, Shanghai 200237, PR China. E-mail: jlhua@ecust.edu.cn

^bDepartment of General Surgery, Sir Run Run Shaw Hospital, School of Medicine, Zhejiang University, Hangzhou 310000, PR China. E-mail: 369369@zju.edu.cn

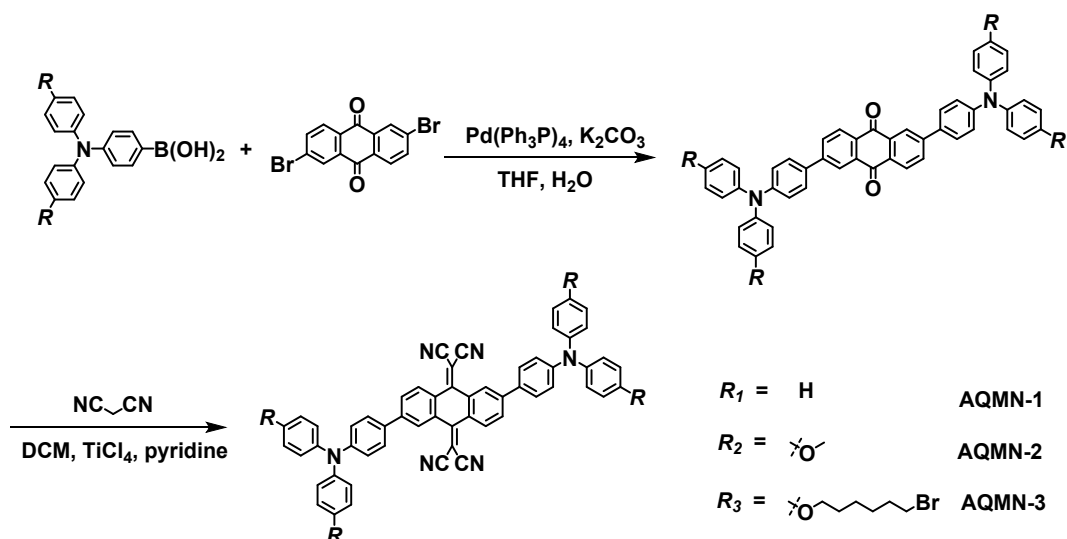
^cState Key Laboratory of Modern Optical Instrumentations, Centre for Optical and Electromagnetic Research, College of Optical Science and Engineering, International Research Center for Advanced Photonics, Zhejiang University, Hangzhou 310058, PR China. E-mail: qianjun@zju.edu.cn

^dMichael Grätzel Center for Mesoscopic Solar Cells, Wuhan National Laboratory for Optoelectronics, Huazhong University of Science and Technology, 1056 Luoyu Road, Wuhan 430074, Hubei, PR China.

‡ Z. Y. and X. F. equally contributed to this work as first authors

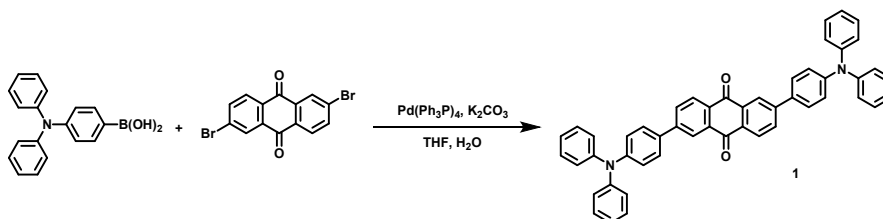
Table of Contents

Section	Title	Pages
Section S1	Synthesis and characterization	S3-S13
Scheme S1	Synthetic route of compounds AQMN-1~3	S3
Fig. S1-13	NMR and HRMS spectra	S7-S13
Section S2	Experimental procedures	S14-S15
Table S1	Molecular orbital distributions and energy optimized in vacuum	S16
Fig. S14-17	Chemical properties of compounds AQMN-1~3	S17-S18
Fig. S18-21	In vitro test of AQMN-1~3 NPs	S19-S20
Fig. S22-25	NIR-II image of AQMN-3 NPs in vivo	S21-S22

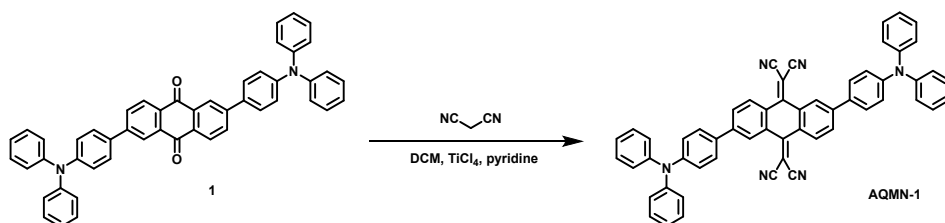


Scheme S1. Synthesis routes of compounds **AQMN-1~3**.

Synthesis of AQMN-1

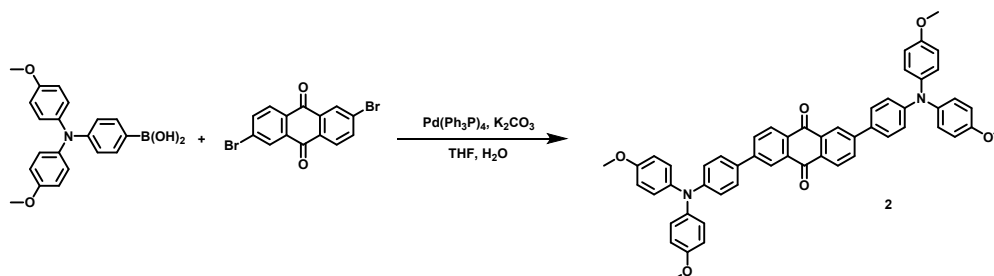


Compound 2,6-dibromoanthracene-9,10-dione (3.62g, 10mmol) and $\text{Pd(PPh}_3\text{)}_4$ (50 mg) were added into a 250 mL two-necked flask, then 100 mL tetrahydrofuran (THF) and 2 mL K_2CO_3 aqueous solution (1 g K_2CO_3 dissolved in 5 mL water) were added. Subsequently, the mixture was stirred at 45 °C for 30 min under the protection of an argon atmosphere. Then 4-(diphenylamino)phenylboronic acid (5.98 g, 20 mmol) was dissolved in THF and added into reaction solution. The mixture was warmed to 70 °C and kept stirring for 8 hours. Solvent was removed under vacuum and the crude product was purified by extraction process by using dichloromethane and water mixture for three times and collected the organic phase. Then the crude product was purified by column chromatography on silica gel using dichloromethane/petroleum (2:1 v/v) as eluent to provide pure product **compound 1** as a red solid (4.8 g, 69.5% yield). $^1\text{H NMR}$ (400 MHz, Chloroform- d) δ 8.52 (d, $J = 1.6$ Hz, 2H), 8.36 (d, $J = 8.1$ Hz, 2H), 7.98 (dd, $J = 8.2, 1.8$ Hz, 2H), 7.63 (d, $J = 8.7$ Hz, 4H), 7.31 (t, $J = 7.8$ Hz, 8H), 7.17 (dd, $J = 8.3, 2.6$ Hz, 12H), 7.09 (t, $J = 7.3$ Hz, 4H).



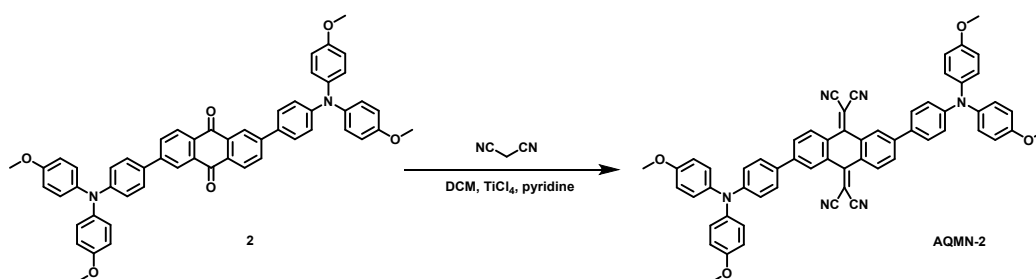
Compound 1 (694 mg, 1 mmol) and malononitrile (264 mg, 4 mmol) were dissolved in 20 mL dichloromethane and the mixture was added into a 50 mL two-necked flask. Then the mixture was stirred at 0 °C for 20 min under the protection of an argon atmosphere. Subsequently, TiCl_4 (92 mmL, 6 mmol) was added and the mixture was kept stirring at 0 °C for 30 min. After that, pyridine (62 mmol, 6 mmol) was added. Then the mixture was warmed up to 40 °C and kept stirring for 4 h. Ice water was added to the mixture dropwise to terminate the reaction. Crude product was purified by extraction process by using dichloromethane and water mixture for three times and then collected the organic phase. Solvent was removed under vacuum and the crude product was purified by column chromatography on silica gel using dichloromethane/petroleum (2:1 v/v) as eluent to provide pure product **AQMN-1** as a green solid (680 mg, 86% yield). ^1H NMR (400 MHz, Chloroform- d) δ 8.42 (d, J = 1.6 Hz, 2H), 8.30 (d, J = 8.3 Hz, 2H), 7.88 (dd, J = 8.3, 1.7 Hz, 2H), 7.54 (d, J = 8.8 Hz, 4H), 7.34 – 7.29 (m, 8H), 7.18 – 7.07 (m, 16H). ^{13}C NMR (100 MHz, CDCl_3) δ 160.51, 149.33, 146.97, 145.13, 131.04, 130.55, 129.52, 128.25, 128.07, 127.36, 125.33, 123.99, 122.49, 113.74, 113.48, 81.79, 77.34, 77.23, 77.03, 76.71. $[\text{M} + \text{H}]^+$ calcd for $\text{C}_{56}\text{H}_{35}\text{N}_6$: 791.2935; found: 791.2923.

Synthesis of AQMN-2



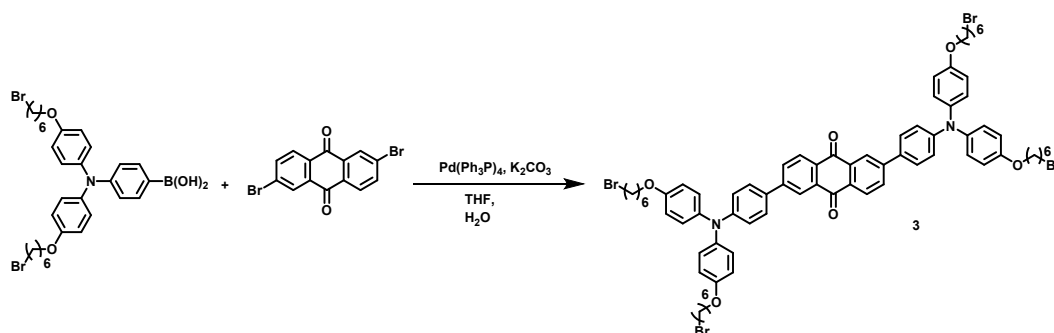
Compound 2,6-dibromoanthracene-9,10-dione (300 mg, 0.82 mmol) and $\text{Pd}(\text{PPh}_3)_4$ (50 mg) were added into a 50 mL two-necked flask, then 20 mL tetrahydrofuran (THF) and 2 mL K_2CO_3 aqueous solution (1 g K_2CO_3 dissolved in 5 mL water) were added. Subsequently, the mixture was stirred at 60 °C for 30 min under the protection of an argon atmosphere. Then (4-(bis(4-methoxyphenyl)amino)phenyl)boronic acid (2.05 mmol, THF solution) was added into reaction solution. The mixture was warmed to 80 °C and kept stirring for 3 hours. Solvent was removed under vacuum and the crude product was purified by extraction process by using dichloromethane and water mixture for three times and collected the organic phase. Then the crude product was purified by column chromatography on silica gel using dichloromethane/petroleum (1:1 v/v) as eluent to provide pure product **compound 2** as a brown solid (220 mg, 32.9% yield). ^1H NMR (400 MHz, Chloroform- d) δ 8.50 (d, J = 1.8 Hz, 2H), 8.33 (d, J = 8.2 Hz, 2H), 7.95 (dd, J = 8.2, 1.8 Hz, 2H), 7.58 (d, J = 8.8 Hz, 4H), 7.12 (d, J = 8.9 Hz, 8H), 7.01 (d, J = 8.8 Hz, 4H), 6.88 (d, J = 8.9 Hz, 8H), 3.82 (s, 12H). ^{13}C NMR (100 MHz, Chloroform- d) δ 183.12, 156.34, 149.61, 146.42, 140.23, 134.16, 131.38, 130.98, 129.90, 128.05, 127.84, 127.11, 124.34, 119.80,

55.49.



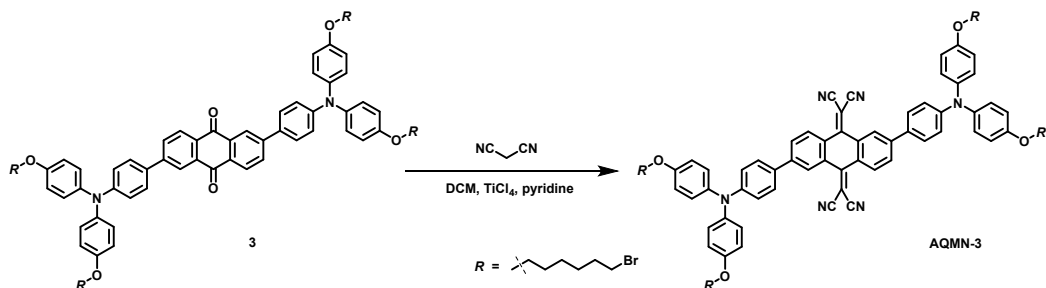
Compound 2 (203.75 mg, 0.25 mmol) and malononitrile (66 mg, 1 mmol) were dissolved in 20 mL dichloromethane and the mixture was added into a 50 mL two-necked flask. Then the mixture was stirred at 0 °C for 20 min under the protection of an argon atmosphere. Subsequently, TiCl₄ (23 mmL, 1.5 mmol) was added and the mixture was kept stirring at 0 °C for 30 min. After that, pyridine (15.5 mmL, 1.5 mmol) was added. Then the mixture was warmed up to 40 °C and kept stirring for 4 h. Ice water was added to the mixture dropwise to terminate the reaction. Crude product was purified by extraction process by using dichloromethane and water mixture for three times and then collected the organic phase. Solvent was removed under vacuum and the crude product was purified by column chromatography on silica gel using dichloromethane/petroleum (2:1 v/v) as eluent to provide pure product **AQMN-2** as a green solid (120 mg, 52.7% yield). ¹H NMR (400 MHz, Chloroform-*d*) δ 8.40 (d, *J* = 1.6 Hz, 2H), 8.27 (d, *J* = 8.3 Hz, 2H), 7.84 (dd, *J* = 8.3, 1.6 Hz, 2H), 7.49 (d, *J* = 8.8 Hz, 4H), 7.12 (d, *J* = 8.9 Hz, 8H), 6.98 (d, *J* = 8.8 Hz, 4H), 6.88 (d, *J* = 8.9 Hz, 8H), 3.82 (s, 12H). ¹³C NMR (100 MHz, CDCl₃) δ 160.60, 156.60, 156.49, 150.17, 145.23, 140.02, 139.86, 131.03, 129.05, 128.58, 128.20, 127.92, 127.36, 126.89, 125.01, 119.48, 114.91, 113.84, 113.61, 81.36, 55.55. [M + H]⁺ calcd for C₆₀H₄₂N₆O₄: 911.3346; found: 911.3334.

Synthesis of AQMN-3



Compound 2,6-dibromoanthracene-9,10-dione (362 mg, 1 mmol) and Pd(PPh₃)₄ (50 mg) were added into a 250 mL two-necked flask, then 100 mL tetrahydrofuran (THF) and 2 mL K₂CO₃ aqueous solution (1 g K₂CO₃ dissolved in 5 mL water) were added. The mixture was stirred at 45 °C for 30 min under the protection of an argon atmosphere. Then 4-(bis(4-((6-bromohexyl)oxy)phenyl)amino)phenyl boronic acid (1.3 g, 2 mmol) was dissolved in THF and added into reaction solution. The mixture was warmed to 70 °C and kept stirring for 8 hours. Solvent was removed under vacuum and the crude product was purified by extraction process by using dichloromethane and water mixture for three times and collected the organic phase. Then the crude product was purified by column chromatography on silica gel using dichloromethane/petroleum (2:1 v/v) as eluent to provide pure product **compound 3** as a brown solid

(320 mg, 21.3% yield). $^1\text{H NMR}$ (400 MHz, Chloroform-*d*) δ 8.49 – 8.24 (m, 4H), 7.92 – 7.82 (m, 2H), 7.54 (dd, $J = 8.9, 4.1$ Hz, 2H), 7.48 (dd, $J = 8.9, 4.1$ Hz, 2H), 7.10 (d, $J = 8.8$ Hz, 8H), 7.02 – 6.94 (m, 4H), 6.86 (d, $J = 8.9$ Hz, 8H), 3.96 (t, $J = 6.3$ Hz, 8H), 3.44 (t, $J = 6.8$ Hz, 8H), 1.96 – 1.85 (m, 8H), 1.85 – 1.76 (m, 8H), 1.56 – 1.48 (m, 16H).



Compound 3 (352.75 mg, 0.25 mmol) and malononitrile (66 mg, 1 mmol) were dissolved in 20 mL dichloromethane and the mixture was added into a 50 mL two-necked flask. Then the mixture was stirred at 0 °C for 20 min under the protection of an argon atmosphere. Subsequently, TiCl_4 (23 mmL, 1.5 mmol) was added and the mixture was kept stirring at 0 °C for 30 min. After that, pyridine (15.5 mmL, 1.5 mmol) was added. Then the mixture was warmed up to 40 °C and kept stirring for 4 h. Ice water was added to the mixture dropwise to terminate the reaction. Crude product was purified by extraction process by using dichloromethane and water mixture for three times and then collected the organic phase. Solvent was removed under vacuum and the crude product was purified by column chromatography on silica gel using dichloromethane/petroleum (2:1 v/v) as eluent to provide pure product **AQMN-3** as a green solid (200 mg, 53.1% yield). $^1\text{H NMR}$ (400 MHz, Chloroform-*d*) δ 8.43 (s, 2H), 8.29 (d, $J = 8.2$ Hz, 2H), 8.18 (d, $J = 8.4$ Hz, 2H), 7.52 (d, $J = 8.8$ Hz, 4H), 7.11 (d, $J = 8.9$ Hz, 8H), 6.99 (d, $J = 8.7$ Hz, 4H), 6.86 (d, $J = 8.9$ Hz, 8H), 3.96 (t, $J = 6.3$ Hz, 8H), 3.44 (t, $J = 6.8$ Hz, 8H), 1.93 – 1.88 (m, 8H), 1.84 – 1.77 (m, 8H), 1.56 – 1.50 (m, 16H). $^{13}\text{C NMR}$ (100 MHz, CDCl_3) δ 156.16, 156.08, 155.97, 139.90, 139.73, 131.06, 127.90, 127.38, 127.26, 127.13, 115.46, 115.43, 99.98, 67.98, 33.84, 32.69, 29.14, 27.94, 25.34. $[\text{M}]^+$ calcd for $\text{C}_{80}\text{H}_{78}\text{Br}_4\text{N}_6\text{O}_4$: 1506.2777; found: 1506.2605.

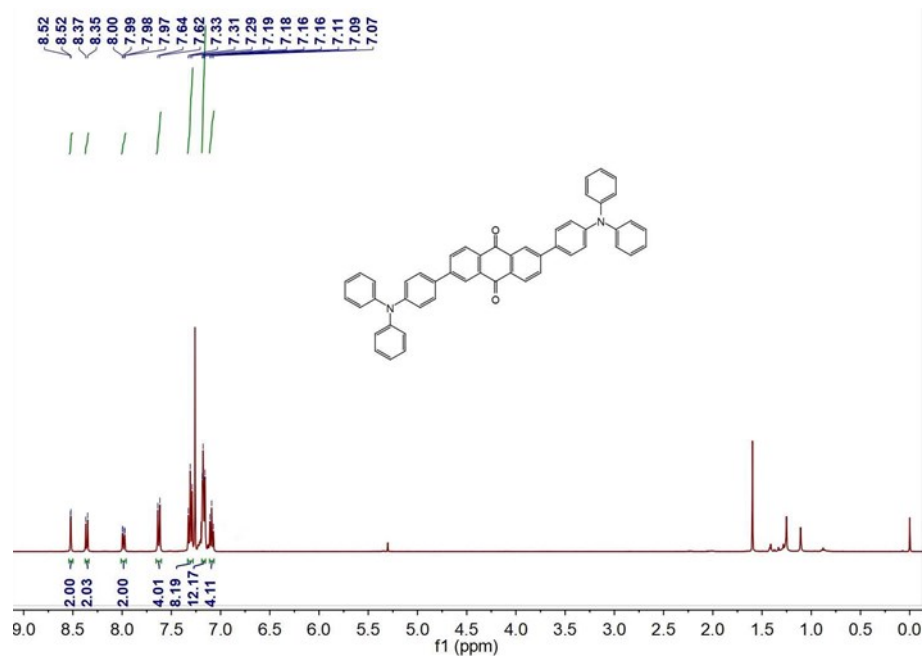


Fig. S1. ^1H NMR spectrum (400 MHz) of intermediate **1** in CDCl_3 .

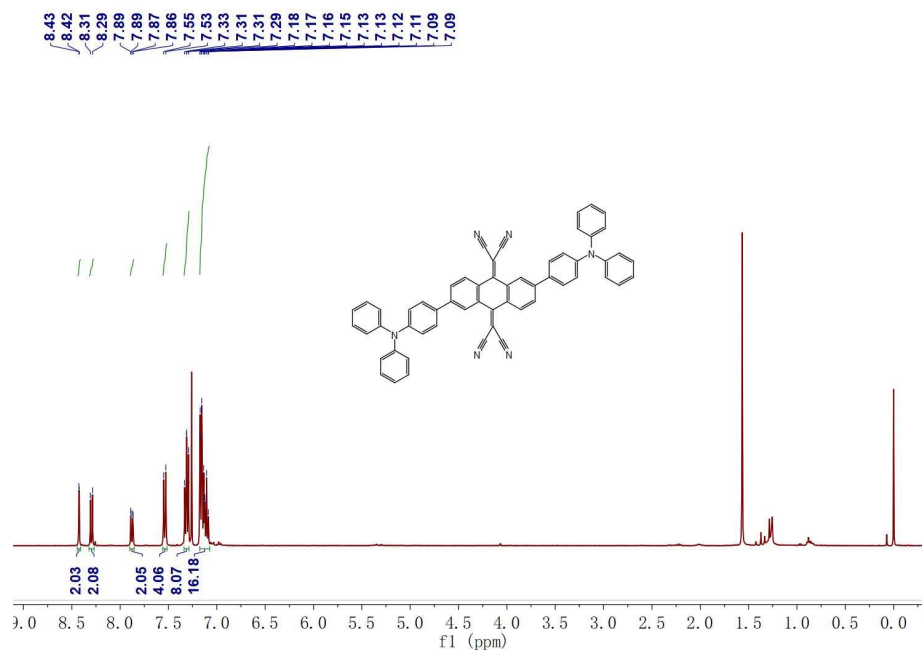


Fig. S2. ^1H NMR spectrum (400 MHz) of **AQMN-1** in CDCl_3 .

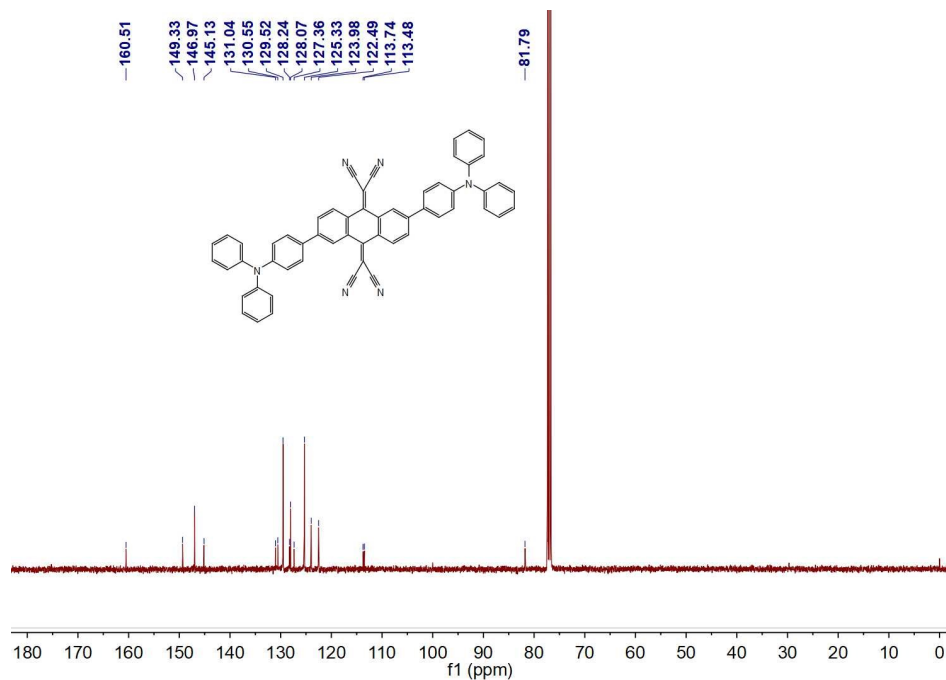


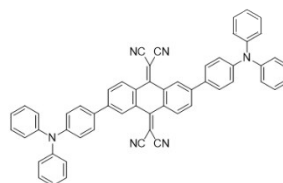
Fig. S3. ^{13}C NMR spectrum (100 MHz) of AQMN-1 in CDCl_3 .

Elemental Composition Report

Single Mass Analysis

Tolerance = 5.0 PPM / DBE: min = -1.5, max = 50.0
 Element prediction: Off
 Number of isotope peaks used for i-FIT = 2

Monoisotopic Mass, Even Electron Ions
 20 formula(e) evaluated with 1 results within limits (up to 50 best isotopic matches for each mass)
 Elements Used:
 C: 0-60 H: 0-50 N: 0-7
 JL-HUA
 HL-LXL-111 4 (0.028) Cm (4)



Page 1

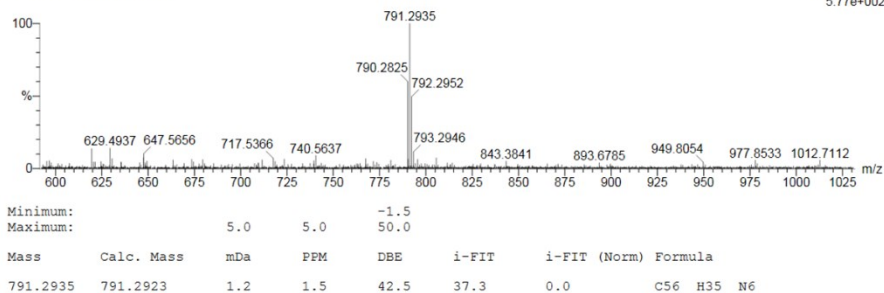


Fig. S4. HRMS of AQMN-1

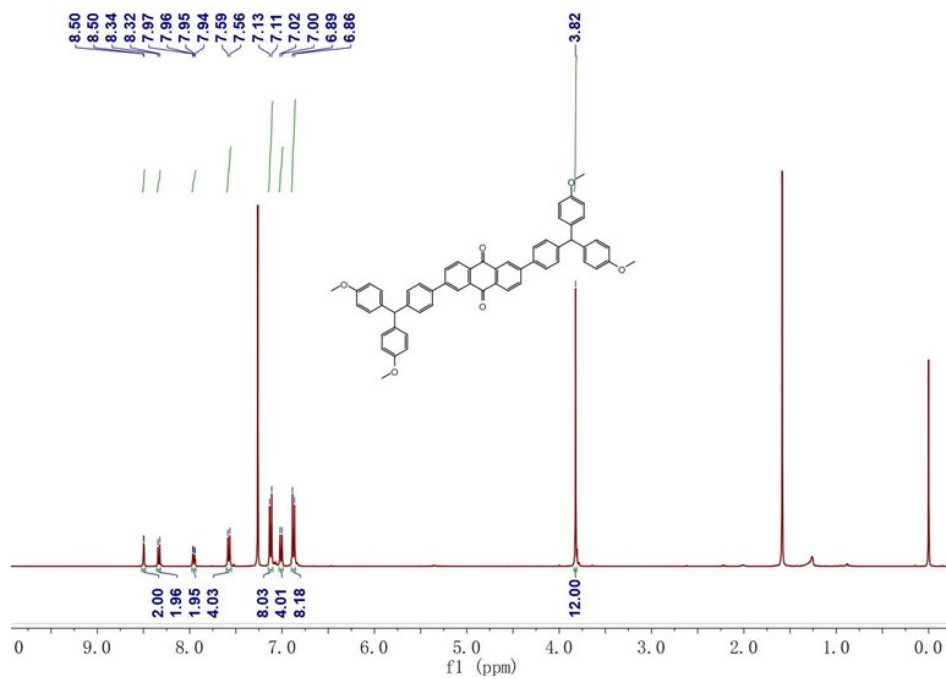


Fig. S5. ^1H NMR spectrum (400 MHz) of intermediate 2 in CDCl_3 .

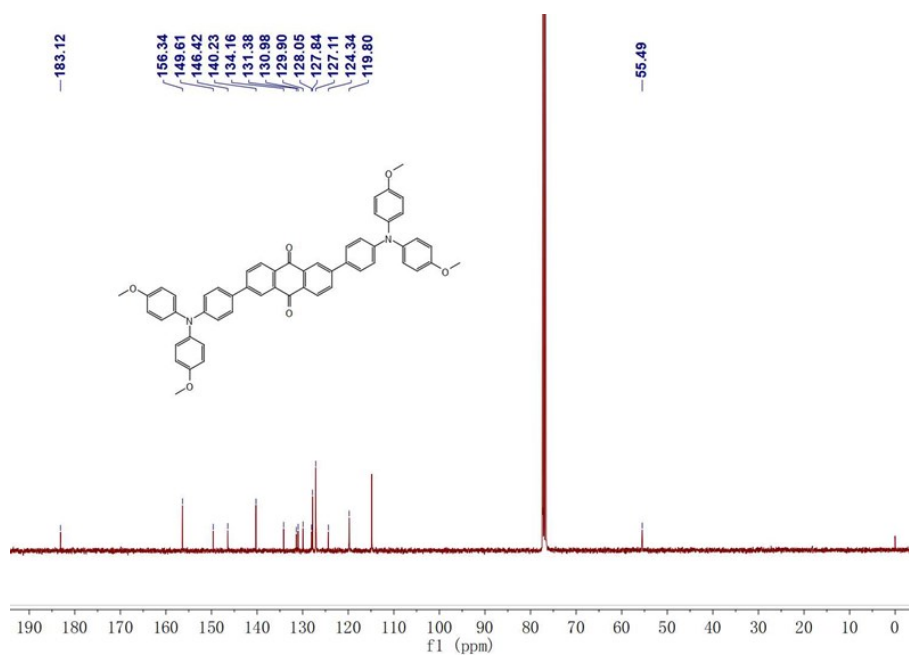


Fig. S6. ^{13}C NMR spectrum (100 MHz) of intermediate 2 in CDCl_3 .

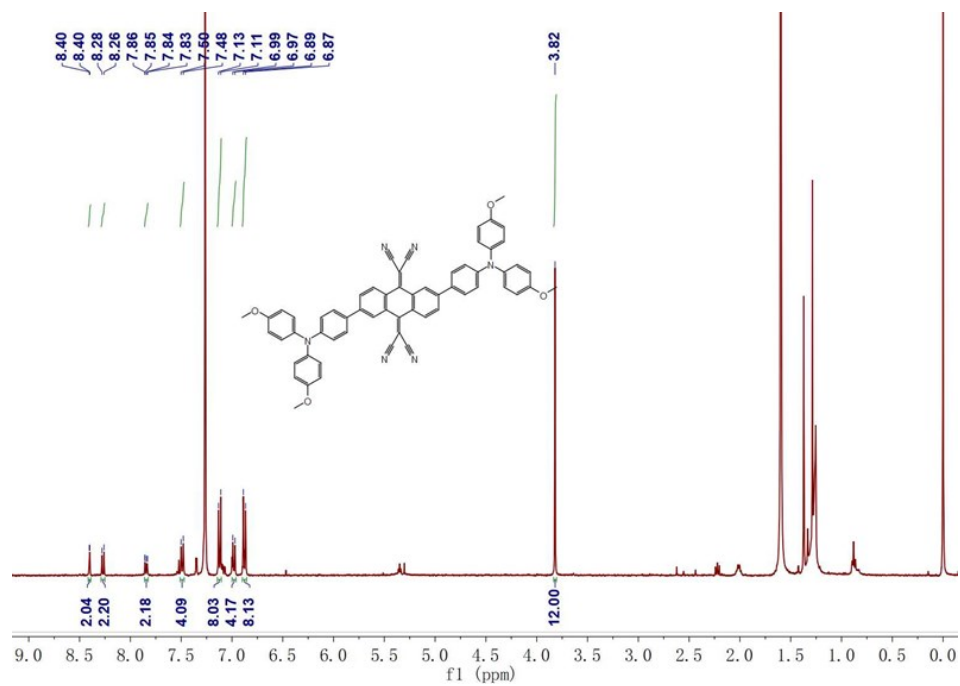


Fig. S7. ¹H NMR spectrum (400 MHz) of AQMN-2 in CDCl₃.

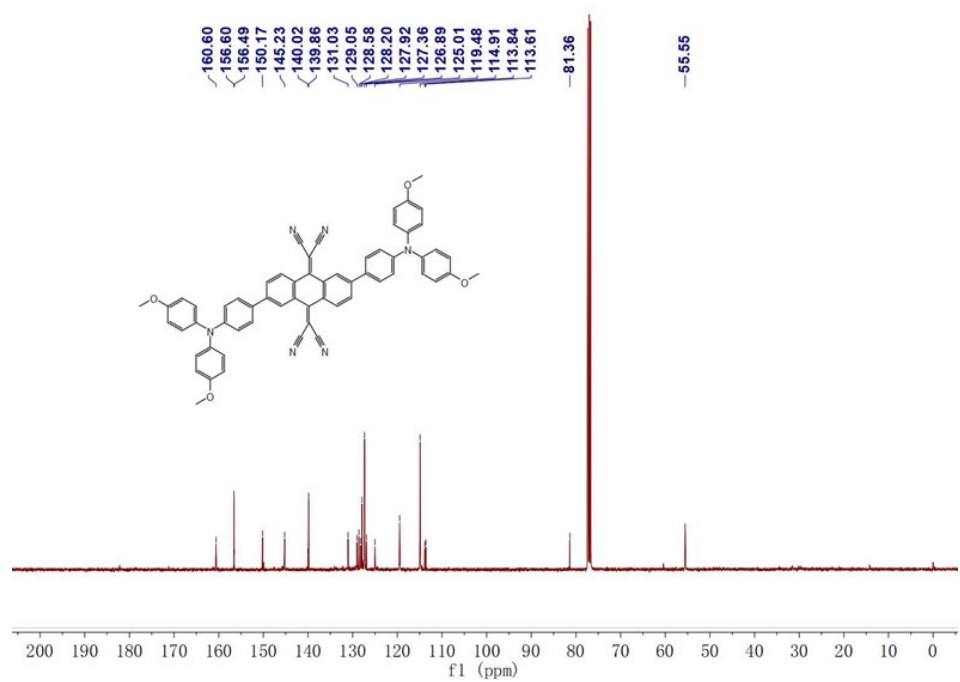


Fig. S8. ¹³C NMR spectrum (100 MHz) of AQMN-2 in CDCl₃.

Elemental Composition Report

Single Mass Analysis

Tolerance = 5.0 mDa / DBE: min = -1.5, max = 50.0

Element prediction: Off

Number of isotope peaks used for i-FIT = 3

Monoisotopic Mass, Even Electron Ions

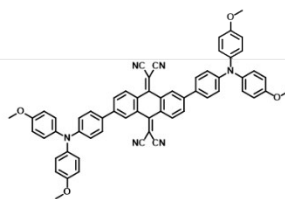
11 formula(e) evaluated with 1 results within limits (up to 50 best isotopic matches for each mass)

Elements Used:

C: 0-60 H: 0-43 N: 0-6 O: 0-4

JL-HUA

HL-YZC-911 118 (1.349) Cm (117.122)



Page 1

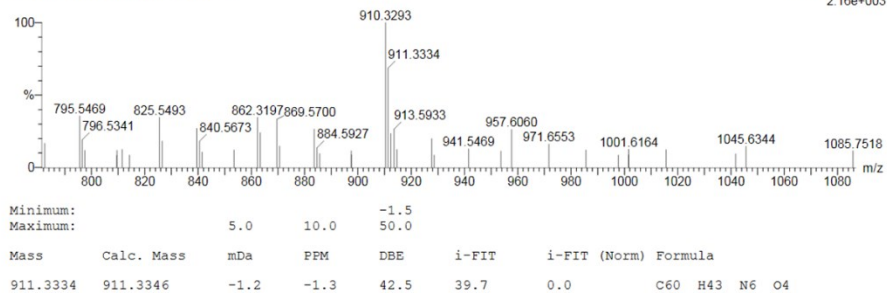


Fig. S9. HRMS of AQMN-2

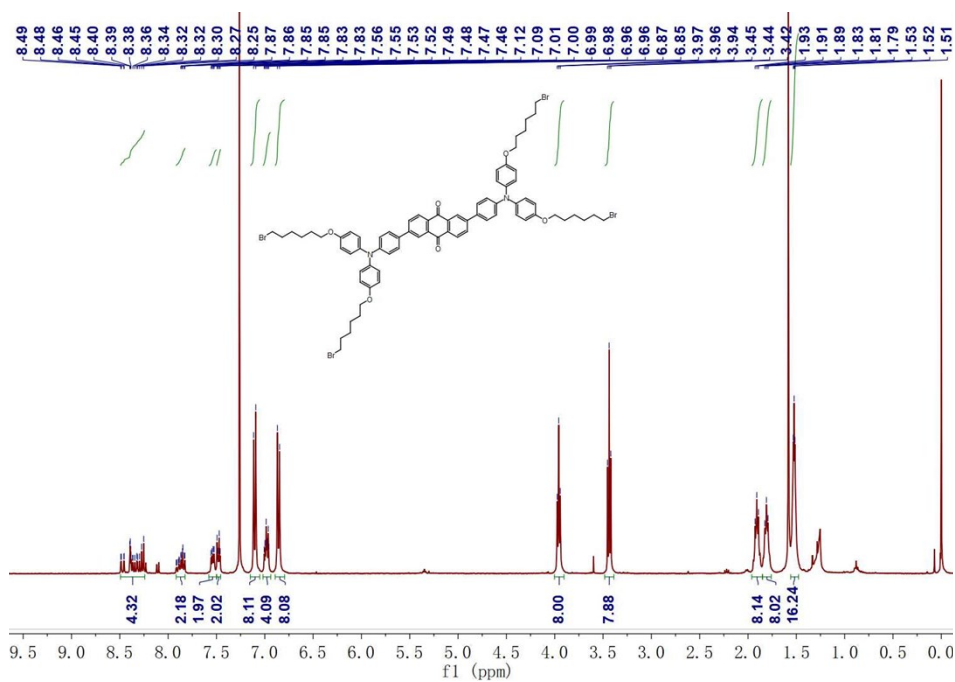


Fig. S10. ¹H NMR spectrum (400 MHz) of intermediate 3 in CDCl₃.

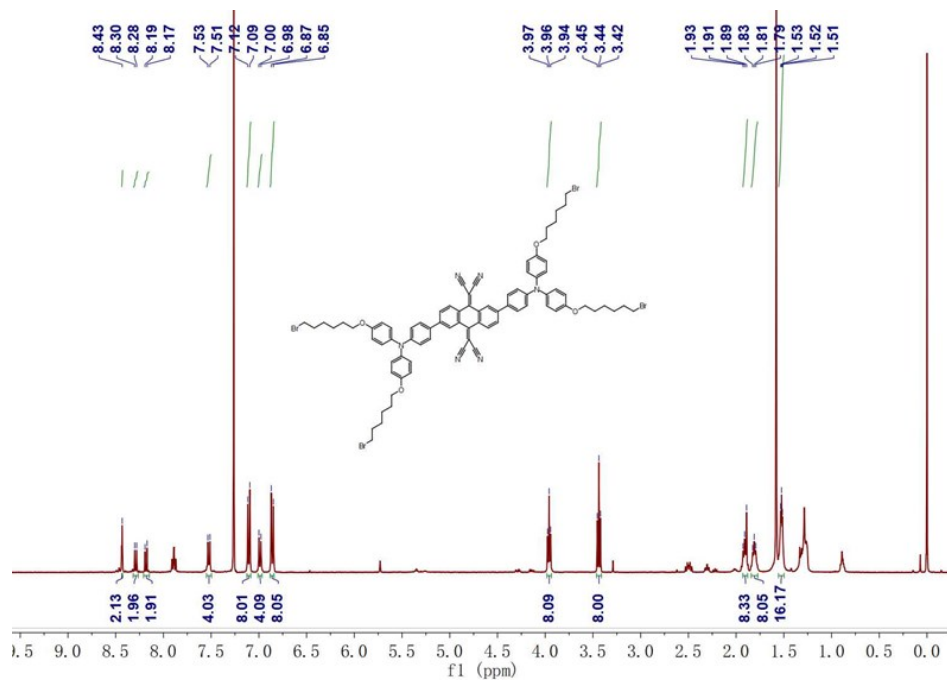


Fig. S11. ^1H NMR spectrum (400 MHz) of AQMN-3 in CDCl_3 .

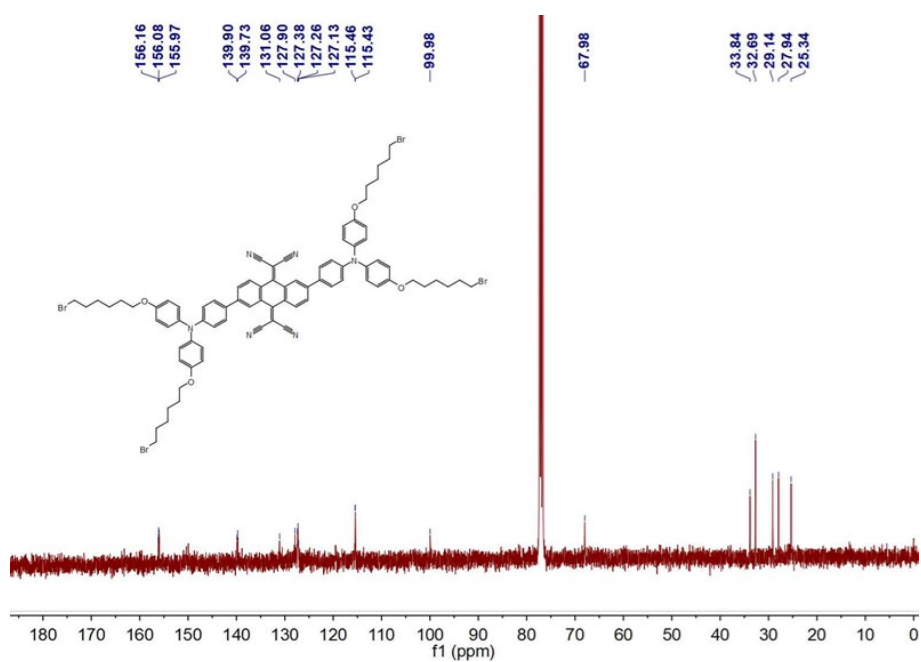


Fig. S12. ^{13}C NMR spectrum (100 MHz) of AQMN-3 in CDCl_3 .

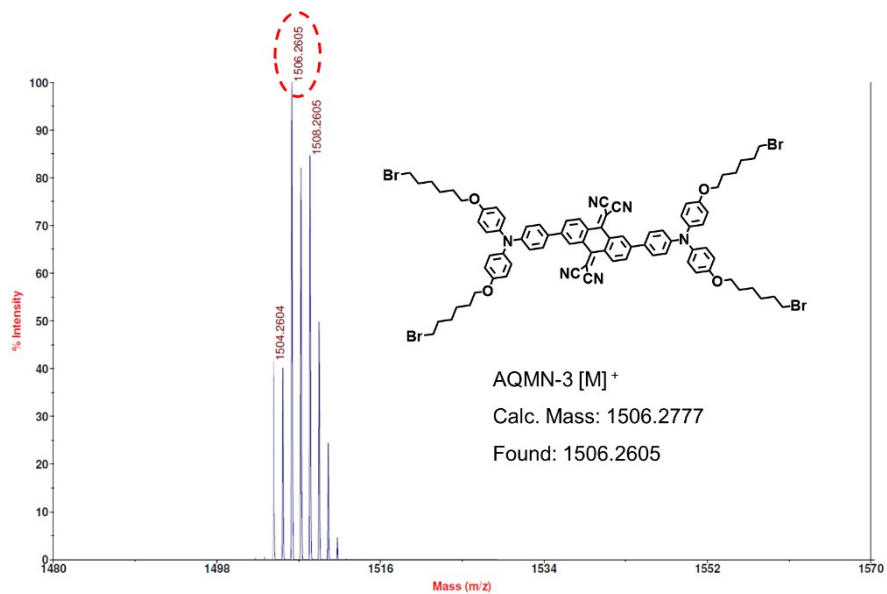


Fig. S13. MALDI-TOF spectrum of **AQMN-3**.

Experimental procedures

Materials

All reagents were bought from commercial sources (Energy Chemical, Sigma-Aldrich, TCI) and used without further processing. All solvents were purified and dried before using by standard methods. The solvents used in spectrum analysis were of HPLC grade. The solutions for analytical studies were pre-pared with deionized water treated using a Milli-Q System (Billerica, MA, USA).

Instruments

¹H NMR and ¹³C NMR spectra were recorded on a Bruker AM-400 MHz NMR spectrometer. Chemical shifts were expressed in ppm (in chloroform-d (CDCl₃) and DMSO-d₆; TMS as an internal standard) and coupling constants (*J*) in Hz. Electrospray ionization and time-of-flight analyzer (ESI-TOF) mass spectra were determined using a Waters Micromass LCT mass spectrometer. Absorption spectra were recorded on a P Varian Cary 500 UV-vis spectrophotometer. The absolute fluorescence quantum yield of the three materials is tested using integrating sphere measurement by Edinburgh Instruments Fluorescence Spectrometer FLS1000. NIR-II imaging of living mouse was collected using an InGaAs camera (TEKWIN SYSTEM, China, 900–1700 nm sensitive) with a 690 nm laser as an excitation.

Density Functional Theory Calculation Methodology

Geometry optimizations were carried out on the molecules in the gas phase, using the software Avogadro [1] to enter the starting geometry. The molecules were distorted to form a variety of conformers which were then allowed to optimize, in order to find the global minimum on the potential energy surface. Frequency calculations were performed on all the optimized geometries to distinguish whether they were minima or transition states on the potential energy surfaces. Where transition state geometries were found, the bond lengths and angles were distorted in the direction of the vibration and the structure was reoptimised until only positive frequencies were obtained. All calculations were carried out using the Gaussian 09 program [2] with the B3LYP functional and UB3LYP [3] and the standard 6-31G(d) basis set. The MO transition assignment was $(CI\ coefficient)^2/0.5*100\%$.

Absorption coefficient of AQMN-1, AQMN-2 and AQMN-3

The absorption coefficient of the three compounds are tested in DMSO (6.67×10^{-6} , 1.33×10^{-5} and 2×10^{-5} M) using the formula $\epsilon = \mathbf{A}/\mathbf{bc}$ (ϵ representing the molar extinction coefficient, **A** representing absorbance, **b** representing length of sample cell, **c** representing concentration of solution). The molar extinction coefficient ($10^4\ M^{-1}cm^{-1}$) of the three compounds are **AQMN-1** 1.48 ($\lambda = 525\ nm$) and 5.89 ($\lambda = 303\ nm$), **AQMN-2** 1.47 ($\lambda = 555\ nm$) and 4.98 ($\lambda = 303\ nm$), **AQMN-3** 1.18 ($\lambda = 549\ nm$) and 4.69 ($\lambda = 296\ nm$). The absorption coefficient spectra are presented in the Fig. S14.

Cytotoxicity of AQMN-1, AQMN-2 and AQMN-3

To evaluate the biocompatibility and security of **AQMN-1**, **AQMN-2** and **AQMN-3**, the cytotoxicity to cancer cells (MCF-7 cells) and normal cells (293T cells and L02 cells) was evaluated by Cell Counting Kit 8 (CCK-8) assays. 293T cells, L02 cells, and MCF-7 cells were seeded in 96-well plates and cultured

in standard 0.2ml DMEM medium containing 10% FBS (Invitrogen, Calsbad, CA, USA) and 1% antibiotics (penicillin, 10 000 U mL⁻¹, streptomycin 10 mg mL⁻¹) for 24 h (37 °C, 5% CO₂). The concentration of AQMN compounds was 0-100 μM. After incubation for 24 h, absorbance was measured at 450 nm using multifunctional microplate reader (Synergy H1, BioTek Instruments, America). The relative cell survival rate (%) was calculated by the following formula: cell survival rate = (OD_{treated}/OD_{control}) × 100%.

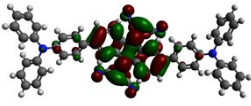
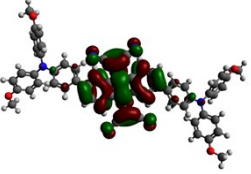
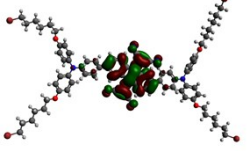
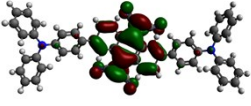
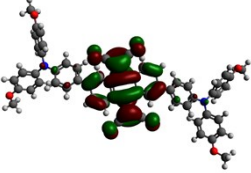
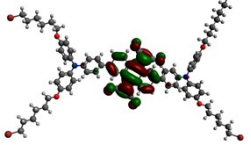
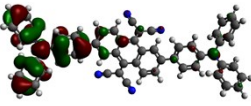
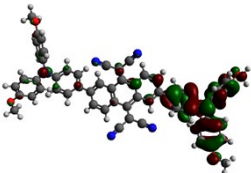
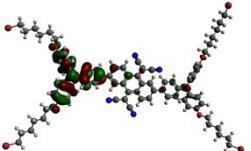
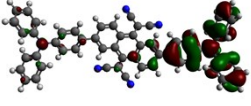
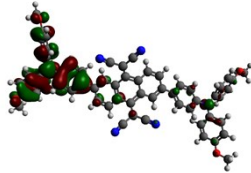
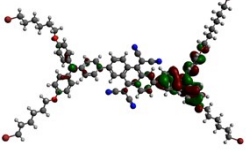
Animals models

The female BALB/c nude mice (6 weeks old) used in this study were obtained from the Laboratory Animal Center of Zhejiang University, and all in vivo experiments were carried out in compliance with the Zhejiang University Animal Study Committee's requirements for the care and use of laboratory animals in research.

Reference

- [1] M. D. Hanwell et al. *J. Cheminform.* 2012, 4, 17.
- [2] Gaussian 09, Revision A.02, M. J. Frisch, G. W. Trucks, H. B. Schlegel, G. E. Scuseria, M. A. Robb, J. R. Cheeseman, G. Scalmani, V. Barone, B. Mennucci, G. A. Petersson, H. Nakatsuji, M. Caricato, X. Li, H. P. Hratchian, A. F. Izmaylov, J. Bloino, G. Zheng, J. L. Sonnenberg, M. Hada, M. Ehara, K. Toyota, R. Fukuda, J. Hasegawa, M. Ishida, T. Nakajima, Y. Honda, O. Kitao, H. Nakai, T. Vreven, J. A. Montgomery, Jr., J. E. Peralta, F. Ogliaro, M. Bearpark, J. J. Heyd, E. Brothers, K. N. Kudin, V. N. Staroverov, R. Kobayashi, J. Normand, K. Raghavachari, A. Rendell, J. C. Burant, S. S. Iyengar, J. Tomasi, M. Cossi, N. Rega, J. M. Millam, M. Klene, J. E. Knox, J. B. Cross, V. Bakken, C. Adamo, J. Jaramillo, R. Gomperts, R. E. Stratmann, O. Yazyev, A. J. Austin, R. Cammi, C. Pomelli, J. W. Ochterski, R. L. Martin, K. Morokuma, V. G. Zakrzewski, G. A. Voth, P. Salvador, J. J. Dannenberg, S. Dapprich, A. D. Daniels, O. Farkas, J. B. Foresman, J. V. Ortiz, J. Cioslowski, and D. J. Fox, Gaussian, Inc., Wallingford CT, 2009.
- [3] Becke, A. D. *J. Chem. Phys.* 1993, 98, 1372–1377.

Table S1. Molecular orbital distributions and energy optimized in vacuum (isodensity=0.020 a.u.).

	AQMN-1	AQMN-2	AQMN-3
LUMO+1	 -2.504 eV	 -2.342 eV	 -2.403 eV
LUMO	 -3.447 eV	 -3.294 eV	 -3.354 eV
HOMO	 -5.240 eV	 -4.917 eV	 -4.965 eV
HOMO-1	 -5.267 eV	 -4.934 eV	 -4.981

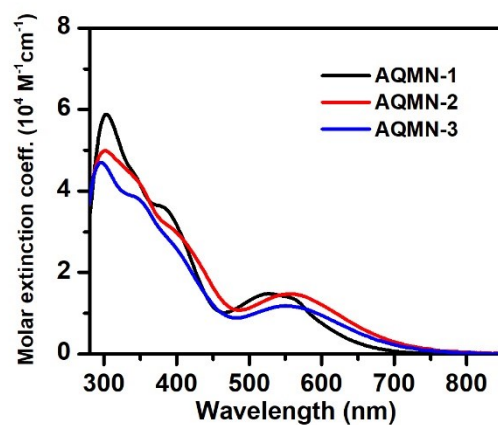


Fig. S14. The absorption coefficient of **AQMN-1**, **AQMN-2**, and **AQMN-3** in DMSO.

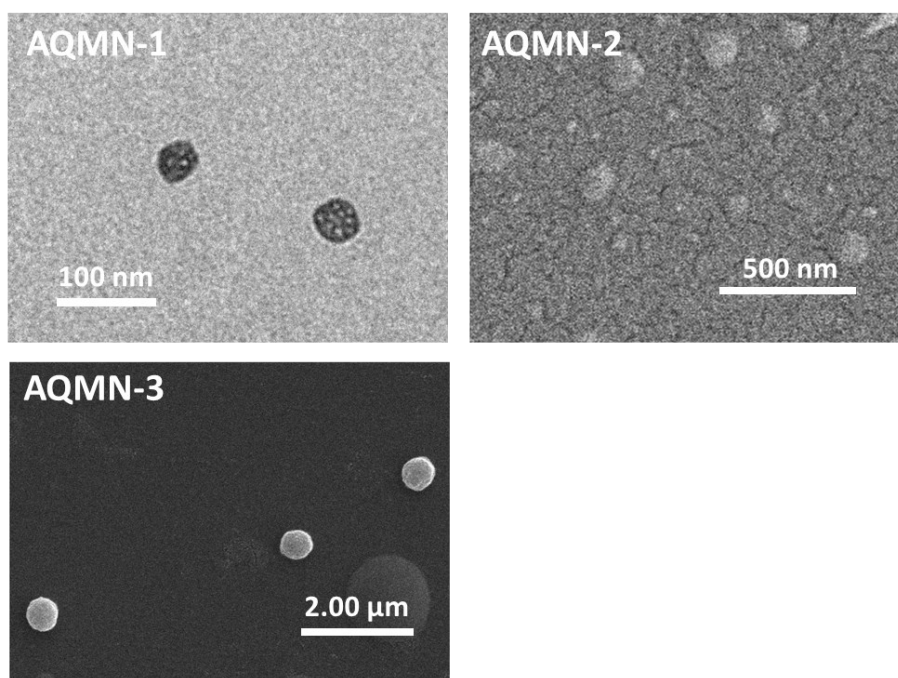


Fig. S15. The representative TEM image of **AQMN-1** in aggregate state (mixture of DMSO: H₂O, v/v = 6:4), SEM image of **AQMN-2** and **AQMN-3** in aggregate state (mixture of DMSO: H₂O, v/v = 2:8).

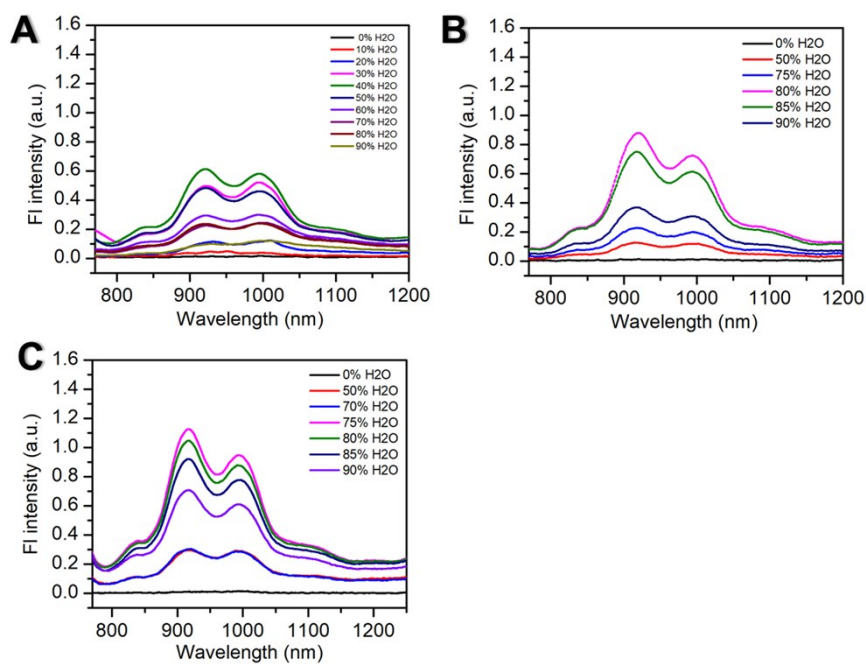


Fig. S16. The fluorescence emission spectra of **AQMN-1** (A), **AQMN-2** (B) and **AQMN-3** (C) in different percentages of H₂O and DMSO.

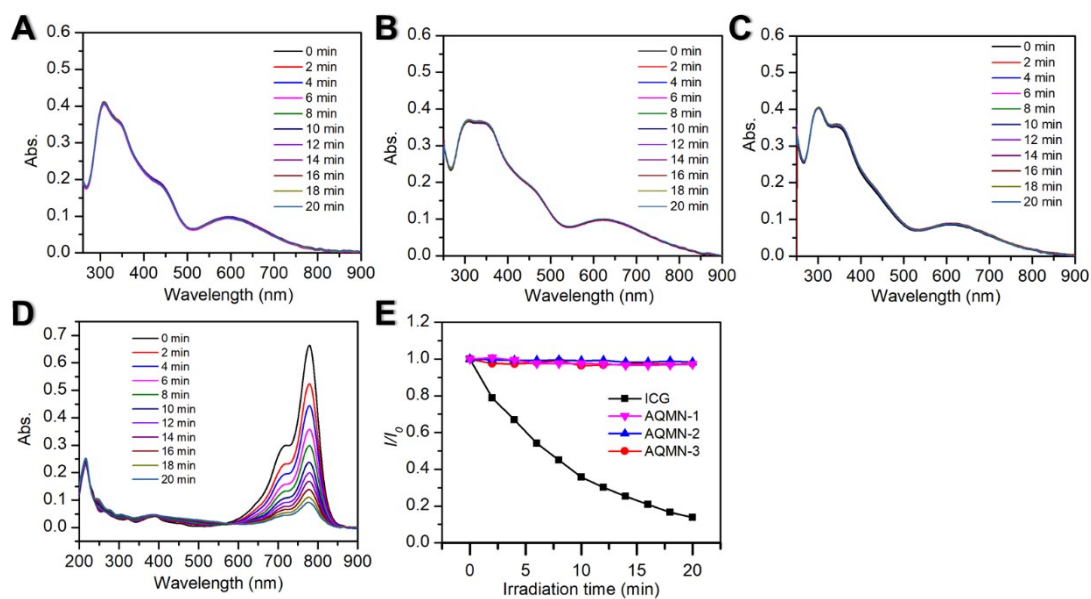


Fig. S17. The photostability of **AQMN-1** (A), **AQMN-2** (B), **AQMN-3** (C) in mixture of DMSO: H₂O (v/v = 2:8) and **ICG** (D) in water (white light, power: 150 mW/cm²).

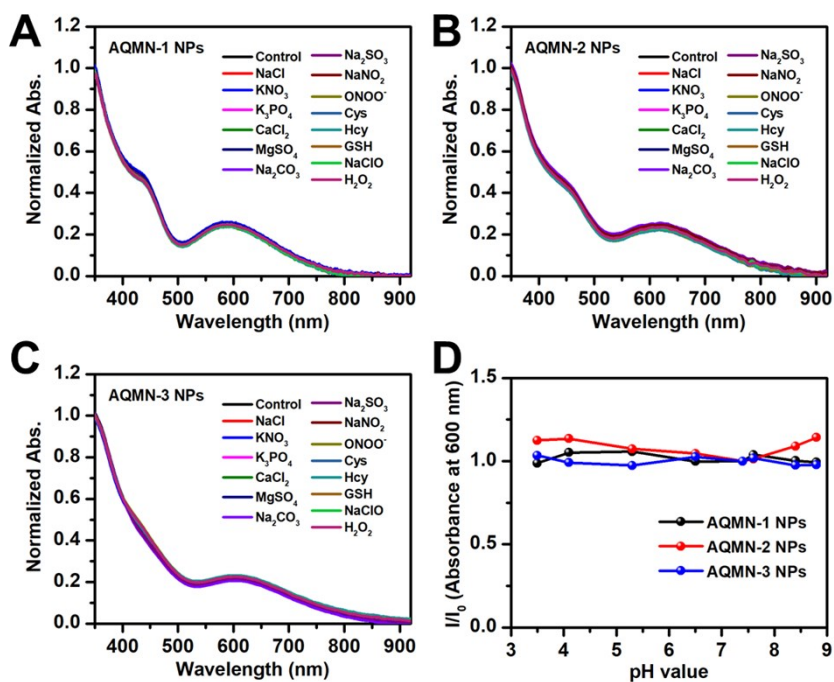


Fig. S18. The chemical stability of AQMN-1 NPs (A), AQMN-2 NPs (B), AQMN-3 NPs (C) in deionized water with the addition of various biological interference. (D) The absorbance of AQMN NPs in different pH PBS buffers (I) at 600 nm comparing to the absorbance in PBS buffers at pH 7.4 (I_0).

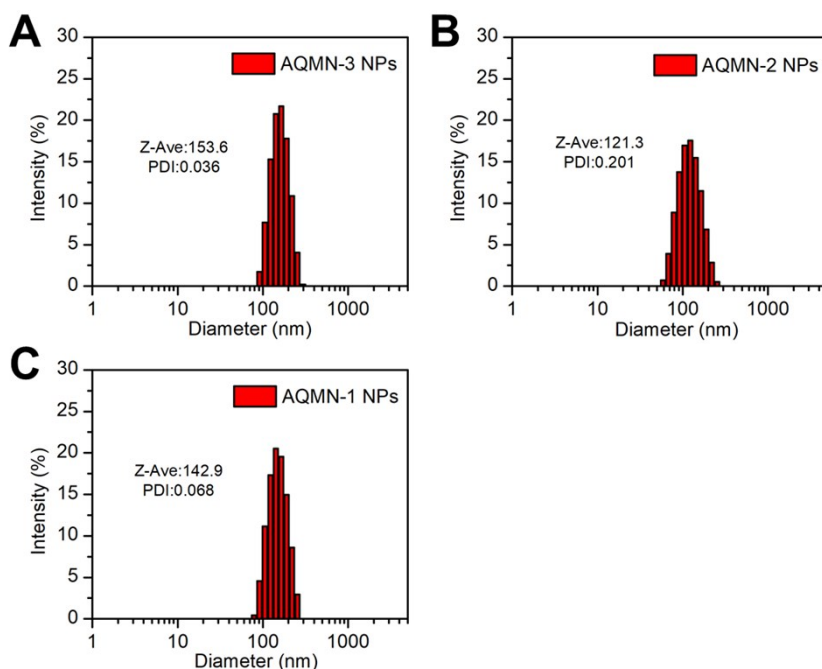


Fig. S19. The diameter of AQMN-1 NPs (A), AQMN-2 NPs (B) and AQMN-3 NPs (C).

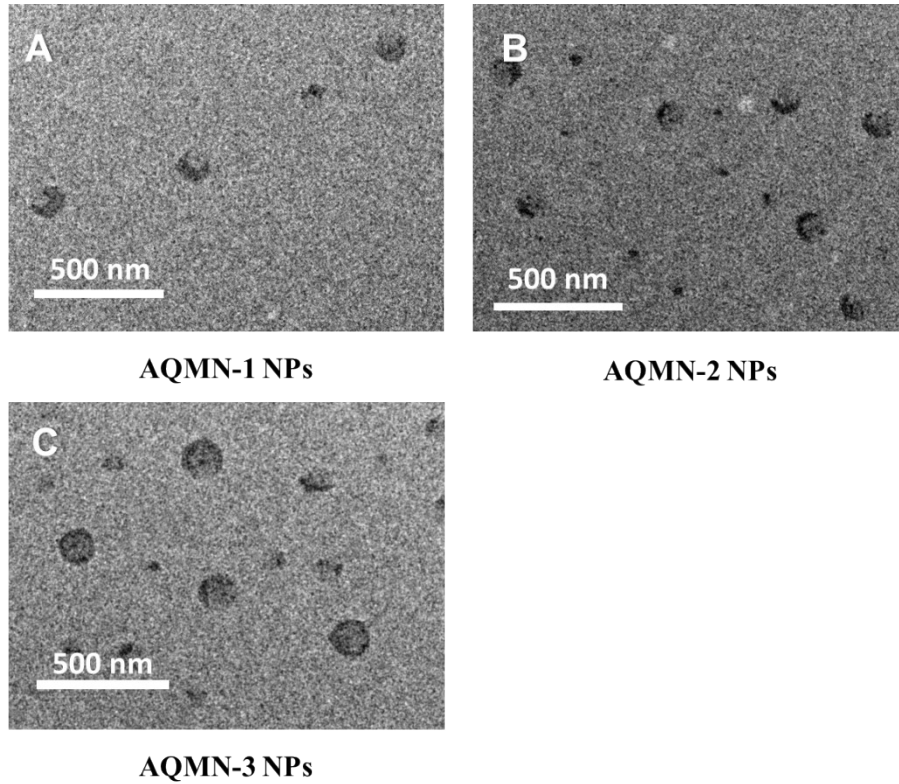


Fig. S20. The representative TEM image of **AQMN-1 NPs** (A), **AQMN-2** (B) and **AQMN-3 NPs** (C).

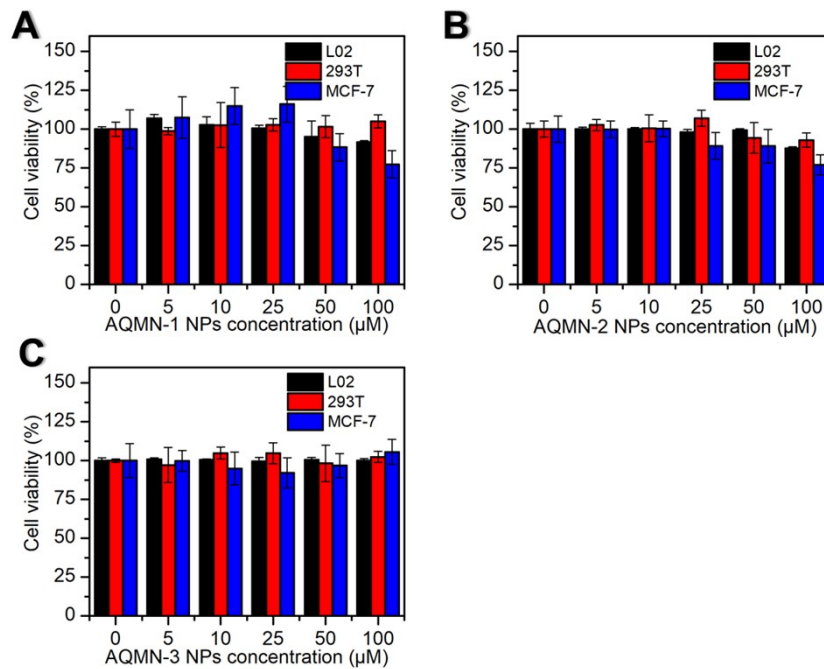


Fig. S21. The viability of **AQMN-1 NPs** (A), **AQMN-2 NPs** (B) and **AQMN-3 NPs** (C) treated L02, 293T and MCF-7 cells in the dark.

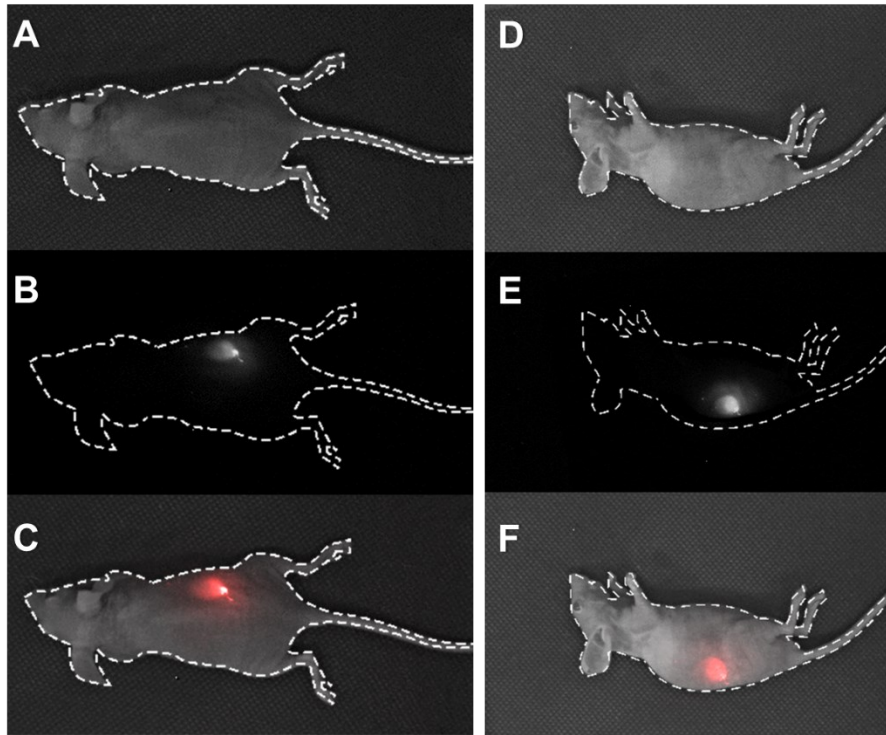


Fig. S22. The NIR-II fluorescence signals of nude mice by subcutaneous injection of **AQMN-3 NPs** (50 μ L, 2 mg/mL).

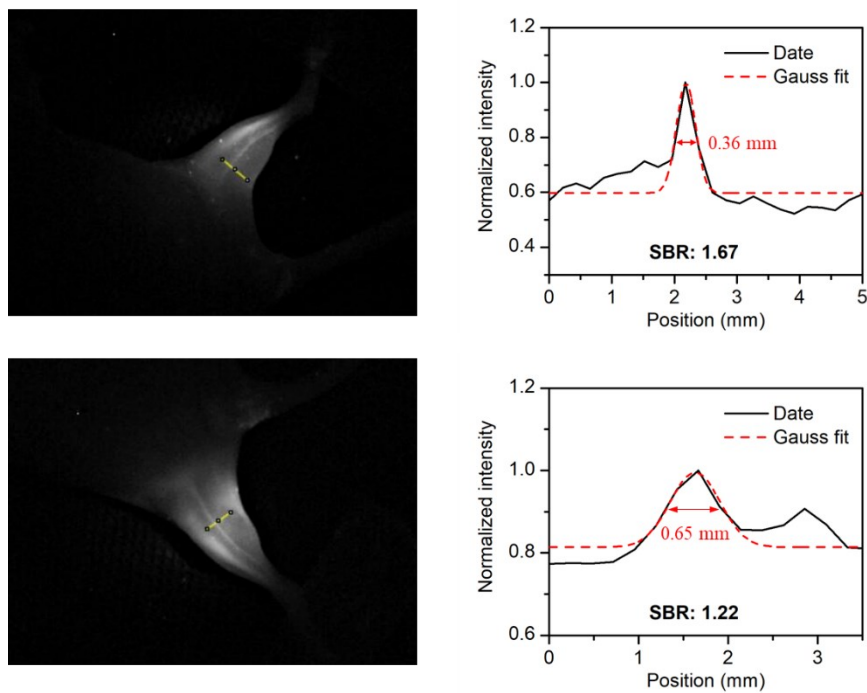


Fig. S23. The NIR-II fluorescence signals for limb femoral vessels imaging of living mice under 900 nm LP filters treated with **AQMN-3 NPs** (250 μ L, 2 mg/mL).

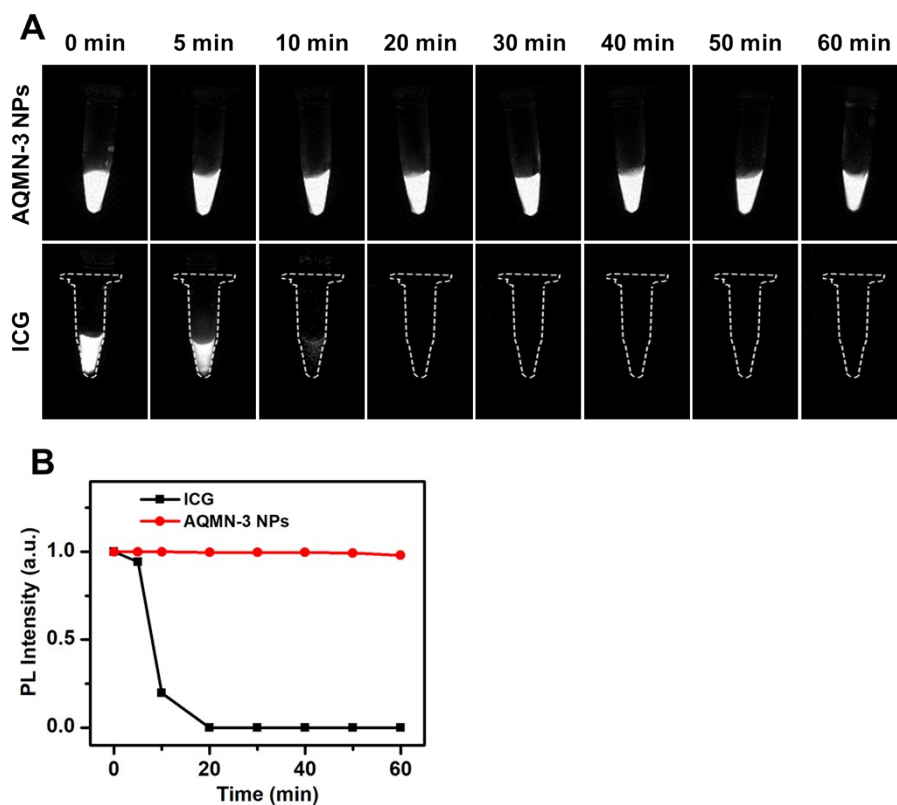


Fig. S24. (A) The NIR-II imaging of **AQMN-3 NPs** and **ICG** after long time irradiation (0-60 min). (B) Normalized PL intensity of ICG and AQMN-3 NPs during irradiation. (Irradiation intensity: 1.5 W/cm²)

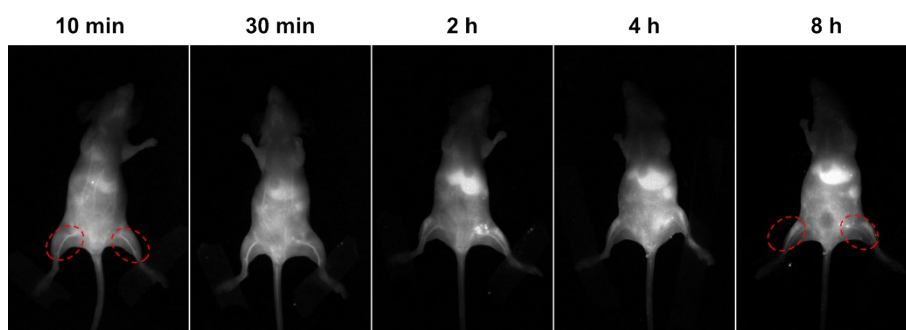


Fig. S25. The NIR-II fluorescence image of the BALB/c nude mice treated with AQMN-3 NPs (250 μ L, 2 mg/mL) by wide-field imaging system upon excitation with a 690 nm laser (power: 100 mW/cm², exposure time: 50 ms, 900 nm LP filter).